IJE TRANSACTIONS A: Basics Vol. 39, No. 10, (October 2026) 2371-2382

International Journal of Engineering

Journal Homepage: www.ije.ir

A Comprehensive Approach to Design of a Temperature Control System in Production Process of Aluminum Alloy Rolled Billets

Y. V. Bazhin, H. D. Tran*

Empress Catherine II Saint Petersburg Mining University, Saint Petersburg, Russia

PAPER INFO

Paper history:
Received 11 September 2025
Received in revised form 26 September 2025
Accepted 13 December 2025

Keywords:
Aluminum Billets
Automatic Control
Continuous Casting and Rolling
Model Predictive Control
Thermal Regime

ABSTRACT

The present work discusses the creation and validation of an automatic control system designed to manage the thermal conditions during the continuous casting and rolling of aluminum billets. At the foundation of this study lies a mathematical model describing heat transfer phenomena in the billet, with particular emphasis on the influence of phase transitions and the release of latent heat during solidification. To ensure the accuracy of the model, experimental temperature data were collected from several points along the crystallizer rolls, providing a reliable basis for comparison. The simulations showed strong agreement with experimental observations, with deviations of less than five percent, which confirmed the robustness of the proposed formulation. Building on these findings, a model predictive control algorithm was incorporated into dedicated software, enabling real-time stabilization of casting and rolling conditions. The results demonstrated clear benefits, including enhanced product quality, improved process stability, and noticeable reductions in energy consumption.

doi: *10.5829/ije.2026.39.10a.02*

Graphical Abstract

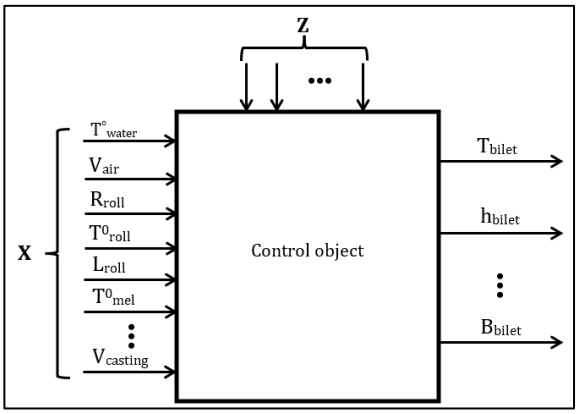

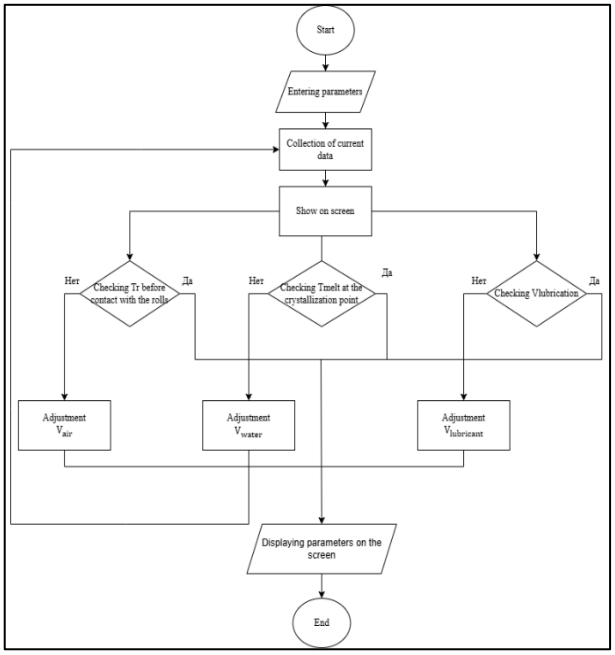

*Corresponding Author Email: hieumd1998hp@gmail.com (H. D. Tran)

Please cite this article as: Bazhin YV, Tran HD, A Comprehensive Approach to Design of a Temperature Control System in Production Process of Aluminum Alloy Rolled Billets. International Journal of Engineering, Transactions A: Basics. 2026;39(10):2371-82.

1. INTRODUCTION

In recent decades, considerable research efforts have been directed toward improving casting and rolling processes for aluminum and other non-ferrous metals. A particular focus has been placed on studies addressing thermal regimes and their impact on the quality of the final product. Numerous investigations have demonstrated that temperature parameters play a decisive role in both the development of microstructure and the formation of defects caused by thermal stresses (1, 2). Huang et al. (3) illustrated the evolution of aluminum alloy microstructures under different casting techniques, enabling a direct comparison between conventional and semi-continuous processes. In their review, Amirkhanlou and Ji (4) discussed the prospects of developing lightweight and high-strength aluminum alloys, but their analysis concentrated primarily on metallurgical aspects without addressing the issues of temperature field control.

In the studies conducted by Ilyushin and Boronko (5), as well as Zaitseva and Semykina (6), particular emphasis is placed on the necessity of introducing intelligent control systems into the aluminum industry. Nevertheless, although these contributions underline the significance of such systems, they remain largely conceptual in nature and do not provide a detailed examination of thermal management under strip casting and rolling conditions.

Over the past years, the theoretical basis for modeling thermal processes during metal solidification and deformation has advanced considerably. Brodova et al. (7) investigated phase–structural transformations under extreme conditions, while Churyumov and Pozdnyakov (8) focused on modeling the evolution of microstructure during hot plastic deformation. These studies established an important foundation for further analysis, yet they remain distant from addressing the practical challenges of real-time temperature control in industrial settings. In addition, Delouei et al. (9) and Avramenko et al. (10) proposed comprehensive mathematical models of unsteady heat transfer, which, however, have not yet been integrated into applied control systems.

A significant contribution to the advancement of continuous casting theory was made in the review by Thomas (11), which systematized existing models and numerical approaches for simulating heat transfer and deformation processes. Nevertheless, the author emphasized that most of these models were developed for the steelmaking industry and therefore require adaptation for aluminum alloys. In a related investigation, Wang et al. (12) explored the rolling behavior and interfacial phenomena in Cu–Al composite billets, highlighting the significance of understanding thermal distributions in multicomponent systems. Nevertheless, their study did not consider the application of predictive control techniques.

Recent developments have underscored the growing role of artificial intelligence and machine learning in enhancing temperature regulation processes. For example, Song et al. (13) introduced a multimodal deep neural network designed to control temperature during the continuous casting of steel, achieving high predictive accuracy and demonstrating the promise of intelligent computational approaches in this domain. Simultaneously, increasing attention has focused on the combined process of continuous casting followed by rolling, known as Continuous Casting Direct Rolling (CCDR). The effects of different heat treatment strategies on the properties of 6056 aluminum alloy were examined by Zhao et al. (14) during the direct integration of casting and cold rolling. Jiang et al. (15) further explored the microstructural characteristics and corrosion resistance of aluminum sheets produced via CCDR with ultrasonic melt treatment, highlighting the essential role of precise temperature management in attaining uniform structural properties. Collectively, these findings emphasize that effective thermal control is a key determinant of the material's ultimate performance.

An important direction in technological advancement is strip casting, which represents a refined form of continuous casting and rolling. However, the application of such methods to aluminum strip casting has not yet been realized. The production process based on strip casting technology offers significant advantages over conventional manufacturing techniques (16, 17). This approach can be regarded as an improved variation of the continuous casting method. A comparative overview of selected aspects of the two production methods is presented in Table 1.

Comparable conclusions are reported by Hu et al. (18), who provided a review of the application of soft computing techniques in rolling process control. They emphasized that, although significant progress has been achieved in the steel and non-ferrous sectors, research on aluminum remains notably limited. In a related study Sotnik (19) proposed an automated process control architecture for steelmaking, demonstrating the feasibility of integrating real-time models into closed-loop control systems. Nevertheless, the direct transfer of this approach to aluminum alloys is constrained by their distinct thermophysical properties and the specific characteristics of phase transformations.

Although significant scientific progress has been achieved, the development of specialized temperature control systems for strip casting of aluminum remains an unresolved challenge. Existing publications predominantly address either metallurgical aspects and microstructural analysis, mathematical models of heat transfer, or broader issues related to digitalization and

TABLE 1. Comparative technical parameters of continuous casting and rolling and conventional methods

Criteria	Continuous casting and rolling method	Conventional method
Freezing rate (°C/s)	1 - 10	50 - 100
Rolling speed (m/min)	0,05-6	30 - 60
Energy consumption (kWh/ton)	500 - 800	200 - 400
Rolling pressure (MPa)	20 - 100	5 - 50
Surface roughness (Ra, μm)	0,5 - 3,0	1,5 - 5,0

intelligent systems. However, studies that integrate mathematical modeling of thermal processes with predictive control algorithms specifically for aluminum strip casting have not yet been undertaken.

Thus, several critical gaps can be identified:

– a lack of studies addressing the application of model predictive control (MPC) in the aluminum industry, in contrast to the extensively investigated steelmaking processes;

– limited research on thermal regulation specifically within the "melt–roll" zone during continuous strip casting;

– insufficient integration of numerical heat-transfer models and modern control algorithms into unified real-time systems.

An urgent task, therefore, is the development of a mathematical model and a control algorithm capable of capturing the specific features of heat transfer in the melt–roll contact zone and providing reliable temperature predictions over a given time horizon. The present study addresses this gap by proposing a comprehensive framework that combines numerical simulation of heat transfer with phase transformations and latent heat of solidification, alongside the design and software implementation of a predictive control algorithm. The novelty of this work lies in the fact that model predictive control methods are applied for the first time to regulate the thermal regime under the conditions of continuous strip casting of aluminum billets, whereas this aspect has been virtually absent in the existing literature.

2. MATHEMATICAL MODELING OF THERMAL PROCESS

To construct the model, the primary step is to analyze the fundamental physical phenomena occurring during the process. This is an unsteady heat-transfer problem in a variable material medium, where such parameters as specific heat capacity and thermal conductivity depend on temperature and phase state (solid/liquid) (9, 20). Furthermore, the presence of latent heat during solidification introduces nonlinearity into the problem.

To simplify the analysis while maintaining adequate accuracy, the following assumptions are made (21, 22):

– predominantly one-dimensional heat transfer (normal to the contact surface): when the thickness of the cast strip or billet is small relative to its other dimensions and the principal cooling mechanisms act through the contacting rolls or an externally applied cooling spray, through-thickness temperature gradients dominate the thermal response. Under these conditions, one–dimensional formulations capture the principal transient conduction and phase-change behaviour while substantially reducing numerical complexity. This reduction is especially advantageous for parametric studies and real-time control applications where many forward model evaluations are required.

– macroscopic homogeneity with temperature-dependent bulk properties: at the length scales relevant to thermal modelling of casting and rolling (millimeters to centimeters), microstructural details such as grain morphology or particle dispersions can be represented through effective, temperature-dependent thermophysical properties (density, specific heat, thermal conductivity). This homogenization preserves the macroscopic energy balance and latent-heat effects while avoiding the intractable computational cost of resolving microstructural heterogeneity explicitly;

– negligible radiative heat exchange compared to conduction and forced convection: in typical roll-contact casting environments the dominant heat-sink terms are conduction into the rolls and convective cooling provided by water sprays or cooling jackets. Radiative losses become significant only at substantially higher surface temperatures or in the absence of convective cooling. Omitting radiation from the boundary conditions simplifies the model and introduces only minor error for the process conditions examined; radiation terms may be reinstated if future operating points warrant it;

– geometric evolution and interface motion treated via fixed-grid formulations (enthalpy or effective heat-capacity approaches) rather than continuous remeshing of a moving boundary: moving solid–liquid interfaces in metal solidification can be handled accurately and efficiently by enthalpy-based or effective-specific-heat formulations on a fixed computational mesh. These approaches account for latent heat release and interface progression without the overhead of dynamic mesh adaptation, making them well suited for transient simulations coupled with control algorithms.

The general heat conduction equation with a heat source term is expressed as follows (23, 24):

$$\rho , \left(\frac{Di}{d\tau}\right) = div\left(\lambda , grad(t)\right) + q_v \quad (1)$$

where:

ρ – metal density, kg/m³;

t – temperature, °C;

λ – thermal conductivity, W/(m·°C);
Di/dτ– total derivative of enthalpy with respect to time;
q_v – volumetric heat source, W/m³ (including latent heat of solidification). In the two-phase region (between the liquidus and solidus temperatures), average thermophysical properties are applied.

The thermal processes associated with solidification are described by following relations (25, 26):

$$\psi = \frac{V_{cr}}{V_0} \tag{2}$$

$$q_v = q_{cr}, \rho, C, \left(\frac{D\psi}{d\tau}\right) \tag{3}$$

$$C_{eff}(t) = \begin{cases} C_l & t > t_l \\ C(t) - q_{cr}, \left(\frac{D\psi}{d\tau}\right) & t_s < t < t_l \\ C_s = f(t) & t < t_s \end{cases} \tag{4}$$

where:
C_{eff} – effective heat capacity;
ψ – solid fraction ($0 \le \psi \le 1$);
V_s – volume of the solid phase;
V_{cr} – total volume of the crystallizing melt;
q_{cr} – latent heat of crystallization, J/kg;
$D\psi/d_\tau$ – solidification rate of the alloy;
t_s – solidus temperature, °C;
C_l – specific heat capacity of the liquid metal, J/(kg·°C);
C_s – specific heat capacity of the solid metal, J/(kg·°C.

Effective Properties in the Two-Phase Zone (7, 8):

$$C_{eff}(t) = \frac{(C_l + C_s)}{2} + \frac{q_{cr}}{t_l - t_s} \tag{5}$$

$$\lambda_{eff} = \lambda_l, \psi + \lambda_s, (1 - \psi) \tag{6}$$

$$\lambda_s = \varepsilon, \lambda_l(t) \tag{7}$$

$$\rho_{eff}(t) = \rho_l, \psi + \rho_s, (1 - \psi) \tag{8}$$

where:
λ_l , λ_s – thermal conductivity of liquid and solid metal, W/(m·°C);
ε – enhancement coefficient of liquid-phase thermal conductivity due to convective flow;
ρ_l , ρ_s – density of liquid and solid metal, kg/m³.

Generalized unsteady-state heat conduction equation:

$$\rho_{eff}(t), C_{eff}(t), \frac{dt}{d\tau} = div(\lambda_{eff}(t), grad(t)) \tag{9}$$

Heat transfer at the roll surface (27, 28):

$$-k\frac{dT}{dn} = h_w(T - T_w) \tag{10}$$

$$\frac{dT}{dn} = 0 \quad 0 \le \varphi \le 2\pi \tag{11}$$

$$-kr\frac{dT}{dr} = h_{cont}(T - T_x) + h_{ro} \tag{12}$$

$$(T - T_x)\ \frac{\pi}{2} \le \phi \le (\pi - \phi_1) \tag{13}$$

$$-k\frac{dT}{dn} = h_{cont}(T_K - T)\ \ (\phi_1 \le \phi \le \frac{\pi}{2}) \tag{14}$$

where:
hcont – heat transfer coefficient in the contact zone with the molten metal in the sump W/(m²·K);
Tw– roll surface temperature, °C;
n– normal vector to the contact surface;
hw– heat transfer coefficient from rolls, W/(m²·K);
r– roll diameter, m;
φ– roll inclination angle relative to the horizontal, degrees;
hro– Heat transfer coefficient during roll rotation.

Similarity criteria and heat transfer coefficients:

$$Nu = \frac{(f/8)RePr}{1+12\ 7(f/8)^{1/2}(Pr^{2/3}-1)\frac{h_w D_w}{k_w}} \tag{15}$$

$$f = (1\ 821\ log_{10}\ Re - 1\ 64)^{-2} \tag{16}$$

$$Re = \rho_w U D_h / \mu_w \tag{17}$$

$$\mathrm{Pr} = \mu_w C_w / k_w \tag{18}$$

where:
D_w – characteristic dimension, m;
k_w – thermal conductivity coefficient of the melt, W/(m·K);
Pr – Prandtl number;
f – hydraulic friction coefficient;
U – characteristic velocity, m/s;
D_h – hydraulic diameter, m;
C_w – specific heat capacity of the medium, J/(kg·K);
μ_w – dynamic viscosity of the medium, kg/(m·s);
ρ_w – density of the medium, kg/m³;
Re – Reynolds number.

3. EXPERIMENTAL METHODOLOGY

3. 1. Main Equipment used in the Experiment Included crystallizer rolls with internal cooling channels;

– melt feeding system (trough and nozzle);
– forced-air cooling unit;
– water-cooling system comprising a pump, flowmeter, pressure gauges, and thermometers at the inlet and outlet;
– chromel–alumel thermocouples (type K) with a diameter of 1.0–1.5 mm, together with mounting holders and protective tubes (asbestos or ceramic);
– contact thermocouples for roll surface temperature measurements;
– KSP-4 potentiometer;

– data acquisition system with thermocouple inputs and digital input/output channels;
– thermocouple amplifiers/adapters with a cold-junction block;
– mechanical fasteners for thermocouples, as well as thermally conductive adhesives/pastes;
– instruments for measuring sample geometry.

The measurement points and the locations of the thermocouples are presented in Figure 1.
T0–T4: Positions of the installed thermocouples.
Point D: Initial contact between the molten metal and the roll surface.
Point I: Solidification zone where the metal has fully transformed from liquid to solid.
D, I, B1, B2, B3: Temperature measurement locations on the roll surface.

3. 2. Measurement of Strip Temperature T0 (before the nozzle): The thermocouple was positioned along the axial line within the melt supply channel, 10–20 mm from the nozzle exit. To protect the sensor from direct flow, a ceramic sleeve with a diameter of 3–4 mm was used. The thermocouple was secured in a holder with a screw clamp, preventing displacement due to flow fluctuations.

T1 (center of the strip): Thermocouples for melt temperature measurement were enclosed in protective ceramic or asbestos sleeves and fixed in a holder above the casting cavity. The junctions were located 1–2 mm from the metal surface. At the start of casting, the sensor tip was immersed in the liquid metal; after a few seconds, solidification occurred, anchoring the sleeve and sensor within the billet. The external portion of the wires remained outside the metal, guided along the holder from the heated zone and connected to the measurement system.

T2 and T3 (across the strip width): These were installed symmetrically relative to the axis of the feeder nozzle, at a distance of 45–50 mm from the center. T4 (edge of the strip): Positioned 1–2 mm from the edge to capture temperature gradients near the boundary. Its design was similar to that of T1. All thermocouples (T0–T4) were installed before the melt was introduced.

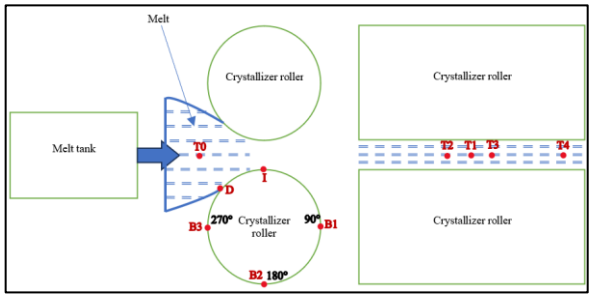

Figure 1. Measurement points and thermocouple locations

Subsequently, the electrical circuit and cold-junction compensation were verified. Measurement uncertainty was ±5 °C.

3. 3. Measurement of Roll-crystallizer Temperature A hole with a depth of 2 mm and a diameter of 3 mm was drilled into the lateral wall of the roll, located 2 mm from the roll surface. A contact sensor was inserted into this hole and fixed using heat-resistant adhesive and a mica spacer. Temperature values were recorded at points in contact with the melt, within the crystallization zone, and after rotating the roll by 90°, 180°, and 270° relative to the crystallization point.

4. ANALYSIS AND VERIFICATION OF THE THERMAL MODEL

Validation of the mathematical model of the thermal regime was performed using the finite difference method (29, 30). This approach relies on discretization of the computational domain, dividing space and time into grid nodes, and replacing derivatives in the governing equations with approximate finite-difference expressions. Instead of solving a complex system of differential equations, the problem is reduced to a set of algebraic equations that can be readily computed (31).

The finite-difference scheme is the central step in modeling transient heat transfer. In the one-dimensional, non-stationary problem considered here, the computational domain is divided into uniform spatial and temporal nodes. The derivatives of the governing differential equation are approximated by algebraic difference formulas for stepwise calculation.

In each grid point, the temperature at the next time step is computed from the current temperature at that point and the temperatures of two neighboring nodes. Explicit schemes were initially applied because of their simplicity and ease of programming. In such a scheme, the update formula for the temperature at node i at time $t + \Delta t$ is given as the current temperature plus the thermal diffusivity term, proportional to the difference between neighboring temperatures, along with the effect of any internal heat source (32, 33).

The thermal diffusivity coefficient α characterizes the rate of heat propagation in the material and is calculated as the ratio of thermal conductivity to the product of density and specific heat capacity. For computational stability—particularly in explicit schemes—the Courant–Friedrichs–Lewy condition must be satisfied, requiring the ratio of the time step to the square of the spatial step to be less than or equal to 0.5. Violation of this condition can lead to oscillations or non-convergence of the numerical solution.

When higher accuracy is required, or when a larger grid step is desirable to reduce computational cost, implicit schemes or the Crank–Nicolson method (a combination of explicit and implicit formulations) can be employed. These methods require solving a system of linear equations at each time step but offer the advantage of unconditional stability (34, 35).

In the numerical implementation, the heat transfer problem was addressed using the finite difference method, which involves constructing a grid of nodal temperature values over the domain of interest. The spatial domain was discretized with a step size of Δx, while the temporal evolution was discretized with a step size of Δt. An explicit scheme was employed to approximate the heat conduction equation:

$$T_i^{n+1} = T_i^n + \frac{\alpha \Delta t}{\Delta x^2}(T_i^n - 2T_i^n + T_{i-1}^n) + \frac{\Delta t, q_v}{\rho, C_{eff}} \quad (19)$$

where:

T_i^{n+1} – temperature at node i at time step n;

$\alpha = \frac{\lambda}{\rho, C_{eff}}$ – thermal conductivity coefficient.

The model was developed in Python, with NumPy handling array and matrix computations, SciPy used to solve the governing equation systems, Matplotlib employed for result visualization, and Tkinter providing the user-interface framework. In the modeling process, parameters such as melt temperature, casting speed, and cooling water flow rate were set according to experimental conditions, while geometric parameters such as roll length, roll radius, and roll gap were fixed. Based on these inputs, the model calculated the temperature distribution along the surface of the crystallizer rolls. Simulation results are presented in Figures 2 and 3.

The roll surface temperature was determined at the initial contact point with the melt (point D), where it reached the maximum range of 440–475 °C. At the crystallization point (point I), the temperature decreased

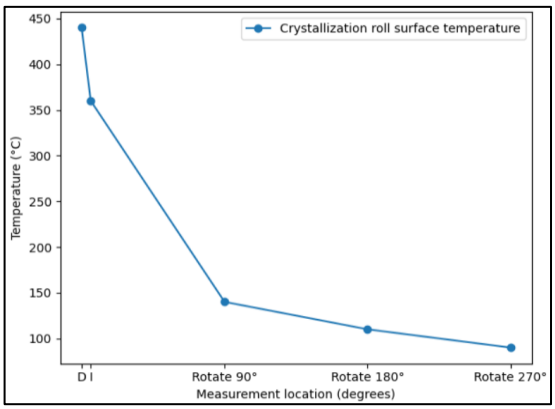

Figure 2. Surface temperature of the crystallizer rolls under lower-bound conditions

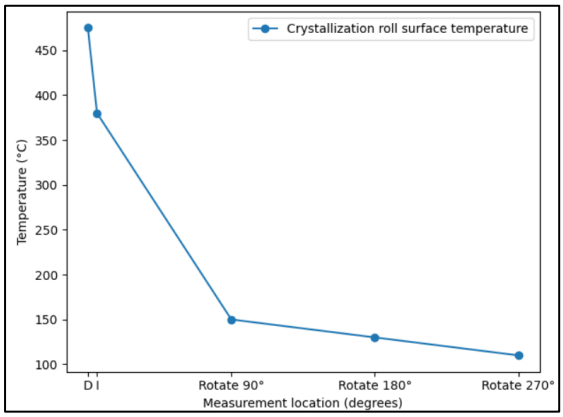

Figure 3. Surface temperature of the crystallizer rolls under upper-bound conditions

to 360–380 °C. As the rolls continued rotation through 90°, 180°, and 270°, the temperature gradually dropped to approximately 145 °C, 120 °C, and 100 °C, respectively. The temperature of the rolled billet was recorded within the range of 445–460 °C.

Table 2 summarizes the comparison of simulated temperatures with experimental values obtained using contact thermocouples at selected points on the roll surface.

The comparison clearly demonstrates that the applied mathematical model provides high accuracy, with a maximum deviation not exceeding 5%, which is acceptable for technical analysis. Such models can be effectively employed in the development of digital control systems as well as for predictive adjustment of process parameters.

5. DESIGN OF THE CONTROL ALGORITHM

The continuous casting and rolling process is characterized by significant transport delay, which complicates control tasks. According to control theory (36, 37), the stability and efficiency of a control system are largely determined by the ratio of delay time (τ) to the time constant of the process (T).

This ratio serves as a criterion for selecting the regulator type and its corresponding control law. When $\tau/T > 0.5$, conventional schemes such as proportional (P), integral (I), proportional–integral (PI), proportional–derivative (PD), or proportional–integral–derivative (PID) often fail to deliver the required system performance (38, 39). In such cases, it is necessary either to reduce the τ/T ratio or to implement more advanced control strategies that incorporate process models. A promising solution is predictive control, where the control action is generated not only on the basis of the current system state but also with regard to the predicted

TABLE 2. Comparison of modeling and experimental results

	Parameter	Experiment	Simulation	ΔT °C	ΔT %
Input data	Melt temperature, °C	680-690			
	Casting speed, mm/s	10-12			
	Cooling water flow rate, L/s	10-15			
	Initial cooling water temperature, °C	25			
	Ambient temperature, °C	25			
	Roll length, mm	1200		-	-
	Roll diameter, mm	800			
	Roll gap, mm	7,6			
	Melt feed rate, kg/s	5-6			
	Initial roll surface temperature, °C	70-90			
	Air cooling rate, m³/s	2			
Output data	Roll temperature at crystallization point, °C	370-400	360-380	15	3.89
	Roll temperature at initial melt contact, °C	450-500	440-475	17.5	3.68
	Roll temperature after 90° rotation, °C	130-175	140-150	7.5	4.92
	Roll temperature after 180° rotation, °C	100-150	110-130	5	4
	Roll temperature after 270° rotation, °C	80-120	90-110	5	5
	Rolled billet temperature, °C	450-480	445-460	12.5	2.69

future behavior of the process. This method offers a significant benefit by incorporating time delays and predicting the future behavior of system parameters, which leads to improved accuracy and stability during actual operation.

For predictive control of the continuous casting and rolling process, the objective function is defined to minimize both the deviation of the actual temperature from the setpoint and the variation of control actions:

$$\min \sum_{i=1}^{N} (T_{act}(t+i) - T_{set}(t+i))^2 + \lambda \sum_{i=1}^{N} \Delta U(t+i)^2 \quad (20)$$

where:

T_{act}— actual temperature;

T_{set}— setpoint temperature, required for compliance with casting specifications, defined by process requirements and entered by the operator via the command module;

$\Delta U(t+i)$— change in the control action (melt feed rate, water or air cooling rate, etc.);

λ— weighting factor balancing tracking accuracy against smoothness of control signals;

N — prediction horizon, typically set to 5–20 steps; here N = 10.

Strict adherence to technological conditions is essential to ensure billet quality. The continuous strip-casting stage consists of three primary phases: melt feeding into the crystallizer rolls, solidification, and lubrication of the cast billet. At the first phase, two key requirements are imposed:

- reduction of melt temperature from 760–800 °C to 680–690 °C;
- melt feed rate onto the rolls maintained at 5–6 kg/s.

In the subsequent phase, the temperature of the semi-solid billet must be decreased from 680–690 °C to 450–480 °C (from roll contact to the solidification point). Finally, continuous lubrication at a rate of 1–2 L/min must be ensured to prevent billet deformation after roll exit.

The control algorithm for the principal parameters of the continuous casting and rolling process is illustrated in Figure 4.

The flowchart uses the following designations:

1. Process start.
2. Input of initial parameters:
   - casting speed V_{cast};
   - water cooling rate V_{water_cool};
   - air cooling rate V_{air_cool};
   - lubricant feed rate $V_{lubricant}$.
3. Collection of real-time sensor data:
   - air and water temperature;
   - melt temperature before roll contact T_r;
   - melt temperature at the solidification point (billet temperature);
   - roll surface temperature;
   - air cooling rate V_{air_cool};
   - lubricant feed rate $V_{lubricant}$;

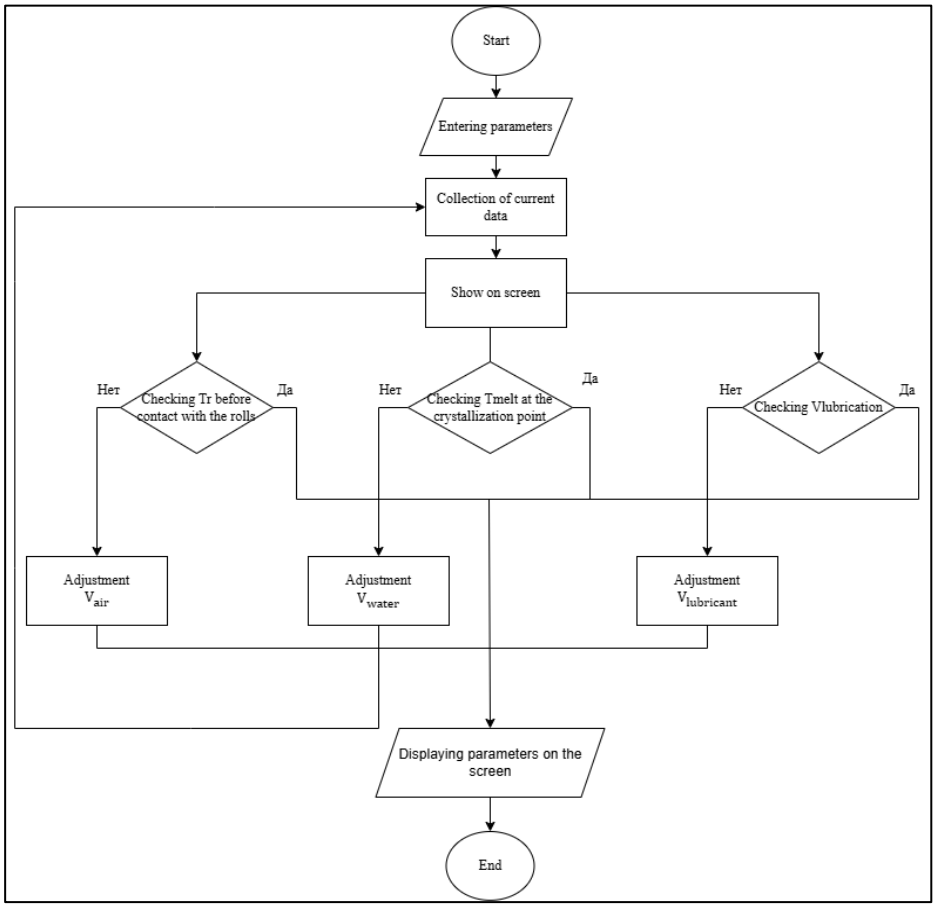

Figure 4. Algorithm for controlling key parameters in the continuous casting and rolling process

4. Real-Time Monitoring and Control of the Strip-Casting Process:
   - the system displays real-time diagrams of the melt temperature before contact with the rolls and at the crystallization point, as well as predicted temperature over the subsequent 10 seconds;
   - the melt temperature before roll contact is maintained within the allowable range of 680–690 °C;
   - at the crystallization point, the melt temperature is controlled within 450–480 °C.
5. Verification of lubricant feed rate.
6. Adjustment of air-cooling rate.
7. Adjustment of water-cooling rate.
8. Adjustment of lubricant feed rate.
9. Process completion and display of final parameters.

6. SOFTWARE IMPLEMENTATION

The continuous casting and rolling process can be represented as a structural control scheme of the managed object, is shown in Figure 5.

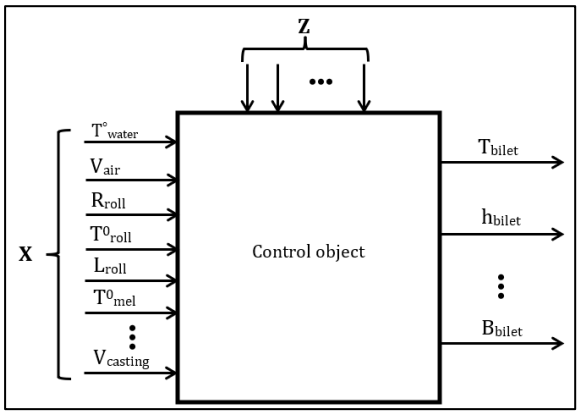

Figure 5. Structural scheme of the continuous casting and rolling process

The input controlled and manipulated parameters X include:
- initial cooling water temperature, T^{0}_{water};
- air-cooling rate in the mixer, V_{air};
- cooling water feed rate to the crystallizer rolls, V_{water};
- casting speed, $V_{casting}$;

− melt temperature before contact with the crystallizer rolls, T^0_{melt};

− initial surface temperature of the crystallizer rolls, T^0_{roll};

− length of the crystallizer rolls, L_{roll};

− melt feed rate, V_{melt};

− radius of the crystallizer rolls, R_{roll}.

Uncontrolled and unregulated input variables Z represent external influences, such as ambient temperature and humidity, voltage stability, and equipment operating consistency.

The outputs correspond to the achieved target parameters, including billet temperature T_{billet}, thickness h_{billet}, width B_{billet}, and surface quality. The structural-functional organization of the continuous casting and rolling process control system is presented in Figure 6.

Drawing on both experimental data and modeling outcomes, a software system was created to regulate the main parameters of the continuous casting and rolling process. Before starting the program, the operator is required to enter the initial process values. The input fields provide suggested default settings that fall within the allowable ranges. An example of the input interface is presented in Figure 7.

When the operator provides inputs that fall outside the recommended limits or are entered in the wrong format, the system issues a warning that calls for correction. Running the equipment with values beyond the allowable ranges can lead to safety risks such as fire, possible equipment malfunction, or unnecessary energy losses. The program will only start once all input parameters are entered correctly. Figure 8 illustrates the input interface in the case of an incorrect entry.

When all input values fall within the permitted range, the system switches to its operating mode. At this stage, the display shows live updates of the selected parameters. Examples of the monitoring interface for the key variables of the strip casting and rolling process, together with real-time graphical outputs, are provided in Figures 9, 10, and 11.

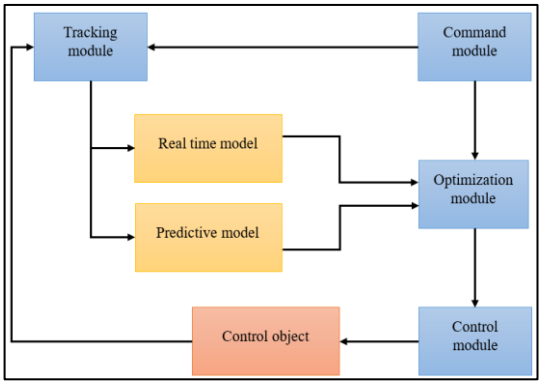

Figure 6. Structural and functional organization of the continuous casting and rolling process control system

Figure 7. Input interface for process parameters

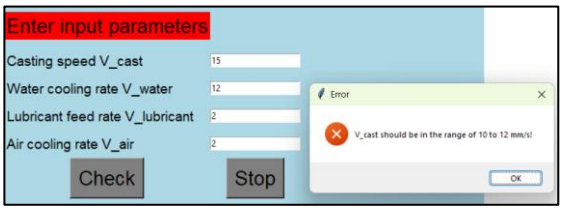

Figure 8. Input interface in the case of an incorrect entry

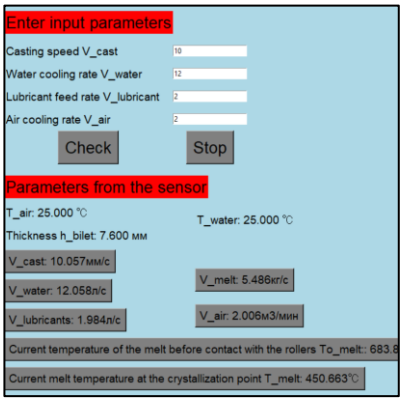

Figure 9. Operational interface of the continuous casting and rolling process control program

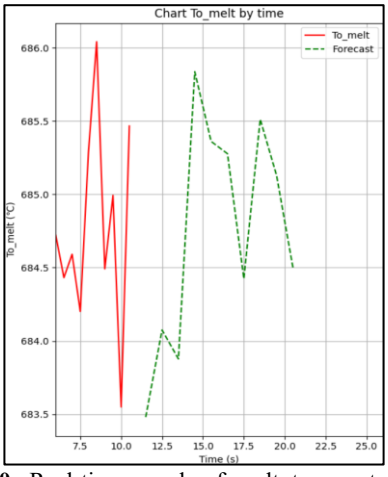

Figure 10. Real-time graph of melt temperature before contact with rolls

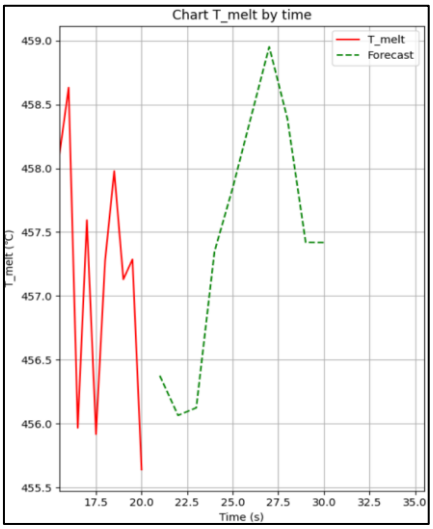

Figure 11. Real-time graph of melt temperature at the crystallization point

The reliability of the system was evaluated using several essential criteria. To begin with, the system blocks initiation whenever input values exceed the allowed range, while simultaneously issuing a warning to the operator. In cases where a component malfunctions, the system does not cease functioning entirely; rather, it switches to a safe operating mode and notifies the operator. Furthermore, even when substantial variations occur during the process, the accuracy of the displayed information remains unaffected, with data being refreshed promptly.

7. CONCLUSION

The conducted study demonstrates that the application of model-predictive control methods in the continuous casting and rolling of aluminum billets represents a promising approach for improving product quality and enhancing the energy efficiency of the technological process. The developed mathematical model and control algorithm confirm the feasibility of integrating numerical simulation of thermal processes with a real-time automatic regulation system. The practical value of these findings lies in the proposed method's ability to mitigate defects caused by thermal instabilities while offering greater adaptability to external disturbances. The developed software also provides a basis for advancing the digital transformation of production lines and incorporating elements of "smart manufacturing" within the aluminum industry.

Nevertheless, the study has certain limitations. The model is largely based on a one-dimensional heat transfer approximation and does not fully consider the effects of complex roll geometries or the heterogeneous microstructure of the alloy. Moreover, the predictive control algorithm is limited by its forecast horizon and would benefit from optimization to improve computational efficiency. Future research should focus on developing multidimensional models of heat and mass transfer, integrating machine learning methods for adaptive control parameter tuning, and creating comprehensive digital twins for production systems.

Acknowledgements

The authors sincerely thank Saint Petersburg Mining University for providing the necessary facilities and academic support to conduct this research. The author(s) also acknowledge the helpful discussions and guidance from colleagues in the related laboratories and departments.

Funding

This research received no external funding and was conducted with institutional support and resources.

Ethics Approval and Consent to Participate

This article does not involve any studies with human participants or animals performed by any of the authors. Therefore, ethics approval and consent to participate are not applicable.

Competing Interests

This article has no conflict with studies by other authors in this field.

Data Availability

The data that support the findings of this study are available upon reasonable request.

Declaration of Generative AI and AI-assisted Technologies in the Writing Process

During the preparation of this manuscript, the authors used ChatGPT (generative AI) exclusively for minor language editing and readability improvement. After using this tool, the author(s) carefully reviewed and edited the content as needed and take full responsibility for the content of the published article.

REFERENCES

1. Boczkal S, Augustyn B, Hrabia-Wiśnios J, Kapinos D, Lewis G, Bareel P-F, et al. Preparation of High-Quality 6xxx Aluminium Eco Alloys Cast in Billets. Engineering Proceedings. 2023;43(1):23. 10.3390/engproc2023043023

2. Greß T, Glück Nardi V, Mittler T, Schmid S, Buchberger P, Tonn B, et al. Interface formation and characterization of brass/aluminum compounds fabricated through die casting and semi-continuous casting. International Journal of Metalcasting. 2020;14(2):564-79. 10.1007/s40962-019-00387-0
3. Huang SH, Zhu BH, Zhang YA, Liu HW, Guo SL. Microstructure Evolution of AlSn20Cu Alloy Prepared by Conventional Casting and Semi Continuous Casting during Rolling and Annealing. Key Engineering Materials. 2021;904:31-8. 10.4028/www.scientific.net/KEM.904.31
4. Amirkhanlou S, Ji S. Casting lightweight stiff aluminum alloys: a review. Critical reviews in solid state and materials sciences. 2020;45(3):171-86. 10.1080/10408436.2018.1549975
5. Ilyushin YV, Boronko EA. Analysis of Energy Sustainability and Problems of Technological Process of Primary Aluminum Production. Energies. 2025;18(9):2194. 10.3390/en18092194
6. Zaitseva NM, Semykina IY. Intelligent control system for technological complexes of aluminum industry enterprises. Bulletin of the Tomsk Polytechnic University Geo Assets Engineering. 2024;335(11):119-32. 10.18799/24131830/2024/11/4613
7. Brodova IG, Zeldovich, V.I., Khomskaya, I.V. Phase-Structural Transformations and Properties of Non-Ferrous Metals and Alloys under Extreme Conditions. Physics of Metals and Metallography. 2020;121(7)::696–730. 10.31857/S0015323020070025
8. Churyumov AY, Pozdnyakov, A.V. . Modeling the Microstructure Evolution of Metallic Materials during Hot Plastic Deformation and Thermal Treatment. Physics of Metals and Metallography. 2020;121(11):1162-86. 10.31857/S0015323020110030
9. Delouei AA, Emamian A, Ghorbani S, He F. A general unsteady Fourier solution for orthotropic heat transfer in 2D functionally graded cylinders. Mathematical Methods in the Applied Sciences. 2024;47(6):3942-59. 10.1002/mma.9796
10. Avramenko A, Shevchuk I, Dmitrenko N, Kovetska YY, Tyrinov A. Unsteady theory of heat transfer and fluid flow during instantaneous transition to film boiling. International Journal of Thermal Sciences. 2020;153:106345. 10.1016/j.ijthermalsci.2020.106345
11. Thomas BG. Review on modeling and simulation of continuous casting. steel research international. 2018;89(1):1700312. 10.1002/srin.201700312
12. Wang J, Zhao F, Xie G, Hou Y, Wang R, Liu X. Rolling deformation behaviour and interface evaluation of Cu-Al bimetallic composite plates fabricated by horizontal continuous composite casting. Journal of Materials Processing Technology. 2021;298:117296. 10.1016/j.jmatprotec.2021.117296
13. Song GW, Tama BA, Park J, Hwang JY, Bang J, Park SJ, et al. Temperature control optimization in a steel-making continuous casting process using a multimodal deep learning approach. steel research international. 2019;90(12):1900321. 10.1002/srin.201900321
14. Zhao J-R, Hung F-Y, Chen B-J. Effects of heat treatment on a novel continuous casting direct rolling 6056 aluminum alloy: Cold rolling characteristics and tensile fracture properties. Journal of Materials Research and Technology. 2021;11:535-47. 10.1016/j.jmrt.2021.01.037
15. Jiang R, Zhao W, Zhang L, Li X, Guan S. Microstructure and corrosion resistance of commercial purity aluminum sheet manufactured by continuous casting direct rolling after ultrasonic melt pre-treatment. Journal of Materials Research and Technology. 2023;22:1522-32. 10.1016/j.jmrt.2022.12.025
16. Belsky A, Ngyen V, Sheikhi M, Starshaia V. Analysis of specifications of bifacial photovoltaic panels. Renewable and Sustainable Energy Reviews. 2025;224:116092. 10.1016/j.rser.2025.116092
17. Gorlanov ES, Leontev LI. Directions in the technological development of aluminium pots. Записки Горного института. 2024(266 (eng)):246-59.
18. Hu Z, Wei Z, Sun H, Yang J, Wei L. Optimization of Metal Rolling Control Using Soft Computing Approaches: A Review. Archives of Computational Methods in Engineering. 2021;28(2). 10.1007/s11831-019-09380-6
19. SV S. Development of automated control system for continuous casting. Radio Electronics, Computer Science, Control. 2024(2). 10.15588/1607-3274-2024-2-18
20. Matveeva VA, Chukaeva MA, Semenova AI. Iron ore tailings as a raw material for Fe-Al coagulant production. Записки Горного института. 2024(266 (eng)):433-43.
21. Vynnycky M. Applied mathematical modelling of continuous casting processes: A review. Metals. 2018;8(11):928. 10.3390/met8110928
22. Lu J, Liu L, Pan W, Wang W, Dou K. New model for heat transfer of copper roller in twin-roll strip casting to assist experimental and industrial process. International Journal of Thermal Sciences. 2025;213:109826. 10.1016/j.ijthermalsci.2025.109826
23. Huang W, Li J, Liu D. Real-time solution of unsteady inverse heat conduction problem based on parameter-adaptive pid with improved whale optimization algorithm. Energies. 2022;16(1):225. 10.3390/en16010225
24. Imane A, Hamid H, Jawad L, Khalid Z, Abdelaziz O. Numerical solution of unsteady conduction heat transfer in anisotropic cylinders. Journal of Thermal Science and Engineering Applications. 2016;8(3):031013. 10.1115/1.4033467
25. Proell SD, Wall WA, Meier C. On phase change and latent heat models in metal additive manufacturing process simulation. Advanced Modeling and Simulation in Engineering Sciences. 2020;7(1):24. 10.1186/s40323-020-00158-1
26. Dai Z, Wang Z, Zhu J, Chen X, Li Q, Jin Z. Three-dimensional solidification modeling of various materials using the lattice Boltzmann method with an explicit enthalpy equation. Physical Review E. 2024;110(2):025301. 10.1103/PhysRevE.110.025301
27. Lekhov OS. Investigation of the Stress-Strain State of the Roll-Strip System during Wide-Flange Beam Rolling in Universal Beam Mills Part 2. . Proceedings of Higher Education Institutions Ferrous Metallurgy. 2015;57(12):15–9. 10.17073/0368-0797-2014-1215–199
28. Yury I, Martirosyan A. The development of the soderberg electrolyzer electromagnetic field's state monitoring system. Scientific Reports. 2024;14(1):3501. 10.1038/s41598-024-52002-w
29. Barjoee SS, Gendler S. Sustainable illumination: Experimental and simulation analysis of illumination for workers wellbeing in the workplace. Heliyon. 2024;10(24). 10.1016/j.heliyon.2024.e40745
30. Nguyen MP, Ponomarenko T, Nguyen N. Energy transition in vietnam: a strategic analysis and forecast. Sustainability. 2024;16(5):1969. 10.3390/su16051969
31. Mazo A. Fundamentals of theory and methods of calculation of heat transfer [Osnovy teorii i metody rascheta teploperedachi]: textbook. Kazan Kazan University. 2013.
32. Fedorova E, Morgunov V, Pupysheva E. Effect of variation of internal diameter along the length of a rotary kiln on material movement. Non-ferrous Metals. 2024;56(1):28-34. 10.17580/nfm.2024.01.05
33. Simakov AS, Mas'ko, O.N., Nikolaev, M.Yu. . Machine Vision System for Quality Assessment of Quartz Raw Materials. Non-Ferrous Metals. 2025;3:81-8. 10.17580/tsm.2025.03.12

34. Skamyin A, Shklyarskiy Y, Lobko K, Dobush V, Sutikno T, Jopri MH. Impedance analysis of squirrel-cage induction motor at high harmonics condition. Indonesian Journal of Electrical Engineering and Computer Science. 2024;33(1):31-41. 10.11591/ijeecs.v33.i1

35. Shklyarsky YE, Lobko, K.K., Kuznetsova, Yu.N., Vorobyov, M.S. Study of Composite Motor Load in the Presence of Higher Harmonics in Electrical Networks. Energy Proceedings of Higher Education Institutions and Energy Associations of the CIS. 2024;67(4):285-99. 10.21122/1029-7448-2024-67-4-285-299

36. Li G, Wang X, Zhu W. Theoretical and experimental investigation on an integral time-delay feedback control combined with a closed-loop control for an infinitely variable transmission system. Mechanism and Machine Theory. 2021;164:104410. 10.1016/j.mechmachtheory.2021.104410

37. Ai B, Sentis L, Paine N, Han S, Mok A, Fok C-L. Stability and performance analysis of time-delayed actuator control systems. Journal of Dynamic Systems, Measurement, and Control. 2016;138(5):051005. 10.1115/1.4032461

38. George T, Ganesan V. Optimal tuning of PID controller in time delay system: A review on various optimization techniques. Chemical Product and Process Modeling. 2022;17(1):1-28.

39. Zhuo-Yun N, Yi-Min Z, Qing-Guo W, Rui-Juan L, Lei-Jun X. Fractional-order PID controller design for time-delay systems based on modified Bode's ideal transfer function. IEEE Access. 2020;8:103500-10. 10.1109/ACCESS.2020.2996265

Persian Abstract

چکیده

کار حاضر به بحث در مورد ایجاد و اعتبارسنجی یک سیستم کنترل خودکار طراحی شده برای مدیریت شرایط حرارتی در طول ریخته‌گری و نورد مداوم شمش‌های آلومینیومی می‌پردازد. اساس این مطالعه یک مدل ریاضی است که پدیده‌های انتقال حرارت در شمش را توصیف می‌کند، با تأکید ویژه بر تأثیر گذارهای فازی و آزادسازی گرمای نهان در طول انجماد. برای اطمینان از دقت مدل، داده‌های دمای تجربی از چندین نقطه در امتداد غلتک‌های کریستالیزر جمع‌آوری شد و مبنای قابل اعتمادی برای مقایسه فراهم کرد. شبیه‌سازی‌ها با مشاهدات تجربی، با انحراف کمتر از پنج درصد، تطابق قوی نشان دادند که استحکام فرمول پیشنهادی را تأیید می‌کند. بر اساس این یافته‌ها، یک الگوریتم کنترل پیش‌بینی‌کننده مدل در نرم‌افزار اختصاصی گنجانده شد که امکان تثبیت شرایط ریخته‌گری و نورد را در زمان واقعی فراهم می‌کند. نتایج، مزایای آشکاری از جمله افزایش کیفیت محصول، بهبود پایداری فرآیند و کاهش قابل توجه مصرف انرژی را نشان داد.